Introduction of an Electromagnetism Module in LS-DYNA for Coupled Mechanical-Thermal-Electromagnetic Simulations

Pierre L'Eplattenier, Grant Cook, Cleve Ashcraft, Mike Burger, Art Shapiro
Livermore Software Technology Corporation
7374 Las Positas Road, Livermore, CA 94551
Email: pierre@lstc.com

Glenn Daehn, Mala Seth
Dept. of Material Sc. And Eng.
The Ohio State University
477 Watts Hall, 2041 College Road, Columbus, OH 43210

Abstract

A new electromagnetism module is being developed in LD-DYNA for coupled mechanical/thermal/electromagnetic simulations. One of the main applications of this module is Electromagnetic Metal Forming. The physics, numerical methods and capabilities of this new module are briefly presented. This module is then illustrated on different simulations. A first set of simulations corresponds to a ring expansion experiment, which was performed at The Ohio State University, for which the code is compared with experimental results. A second example corresponds to a typical Electromagnetic Metal Forming of a thin metallic sheet.

Introduction

Metal working is traditionally done by the relatively slow motion of fixed tool sets. While much has been accomplished using this forming paradigm, there are persistent problems and process limitations. For example local forming strains are essentially limited to those allowed by the forming limit diagram and it is difficult to avoid wrinkling instabilities. Further, the stress and strain that can be applied to the sheet is rather limited, so only modest strength increases due to strain hardening are available through the forming process. There is rapidly growing interest in Electromagnetic Metal Forming (EMF) as a high velocity forming process, where the force deforming the workpiece is a magnetic one, generated by an electrical current induced in the workpiece by a coil. Here impulse and velocity are the primary variables that are controlled, as displacement is controlled in traditional stamping. Much work has shown that in high velocity forming, local strains can significantly exceed strains available in the FLD [1], wrinkling can be mitigated [2], tool-workpiece impact can induce micro- or nano-scale features as well as shock harden the material [3]. Schemes are being developed that permit the use of EMF as a routine manufacturing operation.

An electromagnetism module is being developed in LS-DYNA in order to perform coupled mechanical/thermal/electromagnetism simulations. EMF is the main application of this development, but many other processes could be simulated, where magnetic pressure induces mechanical stress and deformations and/or joule effect induces a heating process: magnetic metal cutting, magnetic metal welding, very high magnetic pressure generation, rail-gun type apparatuses, computation of the stresses and deformations in various coils, magnetic flux compression, induced heating and so forth.

This module allows to the introduction of a source electrical current into solid conductors, and to compute the associated magnetic field, electric field, as well as induced currents. These fields are computed by solving the Maxwell equations in the Eddy current approximation, which is a very good approximation for the magnetic metal forming like problems. The Maxwell equations are solved using a Finite Element Method (FEM) for the solid conductors coupled with a Boundary Element Method (BEM) for the surrounding air (or vacuum), which thus does not need to be meshed [4]. Both the FEM and the BEM are based on discrete differential forms, using the FEMSTER library developed at the Lawrence Livermore National Laboratory [5], which allows a high accuracy for the solution [6],[7]. These methods are now implemented on solid hexahedral elements and quadrilateral shells, and will soon be extended to tetrahedra, wedges and triangular shells.

The electromagnetic fields give the magnetic "Lorentz" force, which is added to the LS-DYNA mechanical solver thus generating deformation of the conductors. This motion is in turn taken into account in the lagrangian computation of the electromagnetic fields.

The electromagnetic fields also give a Joule heating term, which is added to the LS-DYNA thermal solver. The temperature can in turn be taken into account through an equation of state to get the electromagnetic properties of the materials.

Since the electromagnetism module is fully integrated into LS-DYNA, all the already existing numerous mechanical and thermal capabilities of the code can be used. The electromagnetic fields (current density, magnetic field, electromagnetic force, and so forth) can be plotted using LSPREPOST.

First validation of the module: ring expansion experiment

The electromagnetism solver has already been extensively tested on non-moving conductors with simple geometries where analytical solutions are available (strip line, cylindrical line and double wire). It has also been tested against a ring expansion experiment performed at The Ohio State University [8].

The setup for ring expansion experiments was designed primarily to study the effect of sample cross-section and size on its formability. Figure 1 is a schematic of the setup. It essentially consists of a ring specimen placed around a simple helical solenoid coil connected to the capacitor bank. The current in the coil induces an eddy current in the ring in a direction opposite to the primary current in the coil. This causes mutual repulsion between them resulting in the radial expansion of the ring. The current flowing in the coil rises to 120 kA with a rise time of about 24 μs.

The coil used was a closely wound five-turn solenoid made from ASTM B16 brass wire with a 4.7 mm x 4.7 mm square cross-section. The coil had a pitch of 6 mm and its outer diameter was 5.93 cm. It has been designed to result in an axisymmetric radially outward launch of the ring specimen. This solenoid was potted in urethane. In the experiment used for comparison with the code, the ring was made of AA5754. It had a 6.21cm inner diameter with a nearly square cross section with dimensions 3.98 x 3.91 mm.

A Pearson probe [11] was used for measuring the primary current in the coil. The induced current in the ring specimen was measured with a Rogowski probe [12]. A high speed digital array camera (Cooks Flashcam [13]) was used for estimating the position of the sample vs. time as the ring expanded. A detailed description of these experiments is available elsewhere [14].

A hexahedral 3D mesh for the solenoid and the ring was build with the TrueGrid® mesh generation program. It is presented in figure 2, which shows the system at the beginning and at the end of the simulation. The mesh is composed of 1664 solid hexahedral elements, with 16

elements in the cross section of the ring. It has 2304 BEM faces that are used to compute the surface integrals arising in the BEM method. At the time this paper is written, the BEM matrices are assembled and stored as fully dense matrices, which limits the size of the meshes which can

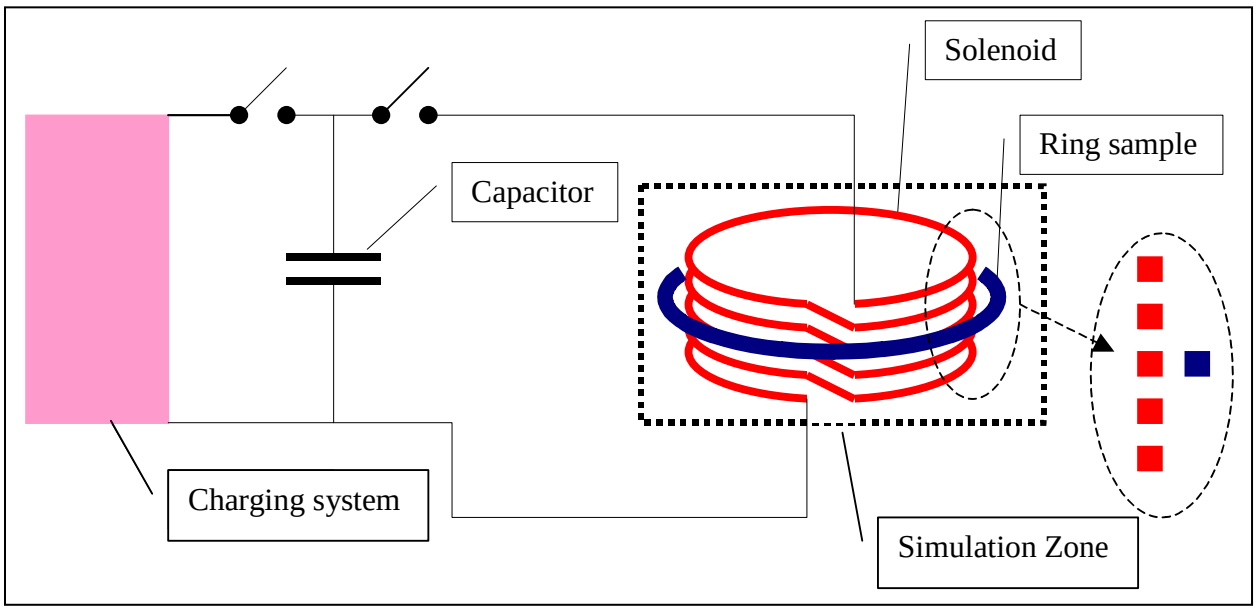

Figure 1: schematic of the setup of the ring expansion experiment

be handled, especially on smaller individual machines. Other methods will be introduced to reduce memory requirements, which should allow using larger meshes.

The measured primary current was injected in the coil and virtual or numerical Rogowski coils permitted computation of the total current flowing through cross sections of both the coil and the ring at each electromagnetic time step of the simulation. These currents are presented on figure 3 along with the corresponding experimental currents.

Since the ring expansion is done at high strain rate (with a peak around 3500 s^{-1}), a material model with strain as well as strain rate dependant stress needs to be used. For this first test, a MAT_24 piecewise linear plasticity was used with the 2 strain rate curves showed on figure 4. The quasi-static one was measured by the OSU team on the exact same material as the one used in the experiment, the one at 2500 m^{-1} was found in [9]. The experimental and numerical ring radius vs time are compared on figure 3, showing very good agreement.

Since the ring expansion experiment nearly has an axi-symmetric invariance, and since it is possible to introduce symmetry planes as well as rotational invariance in the electromagnetic module, another simulation was done with a slice corresponding to 1/16th of the previous simulation zone in the θ direction. The mesh could then be increased in the r and z directions, to 324 elements in the cross section of the ring. This allows study of the diffusion of the current density, magnetic field and of the corresponding electromagnetic force field through the ring. A Burgess equation of state [10] giving the electrical conductivity vs temperature and density was also introduced for the completeness of the model. Figure 5 shows the magnetic field and the force field at three different times during the process. The first time (t=12μs) is during the initial rise of the current, when the magnetic field has not yet diffused much in the volume of the ring. The force is thus mainly applied close the internal face of the ring. The second one (t=33 μs) is after the first peak of the current, during the first half period. The magnetic field has then diffused and the force field is now much more spread through the volume of the ring. One can

notice by the way the pinching effect of the forces. The last time (t=57 μs) is during the second half period when the current has changed sign. This new direction of the current did not have time to diffuse to the center of the ring yet, and the current density does not have the same sign on the internal face as in the center of the ring, as the different rotation directions of the magnetic field show. The corresponding force field is a fairly complicated one, with expanding forces in parts of the volume along with contracting ones in other parts.

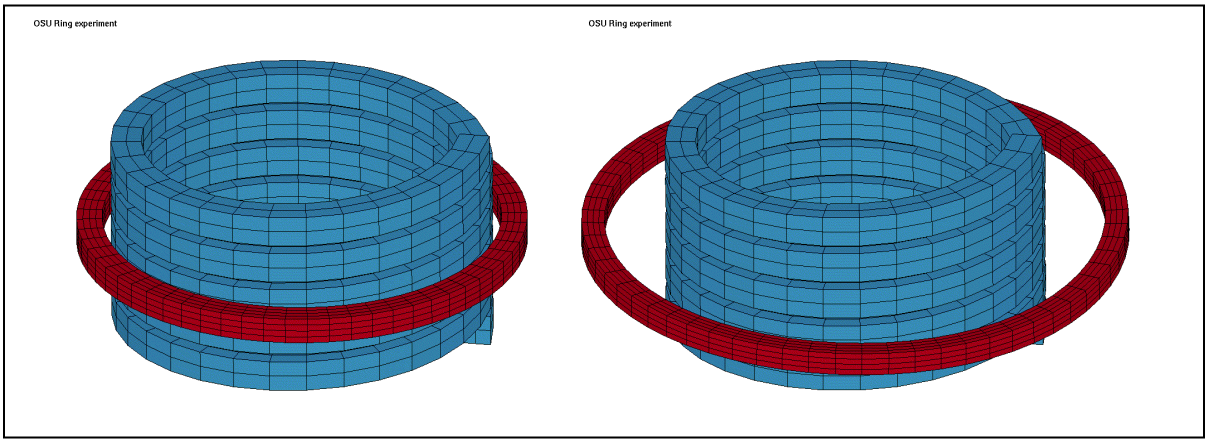

Figure 2: Mesh for the OSU ring expansion experiment at initial stage (left) and final stage (right)

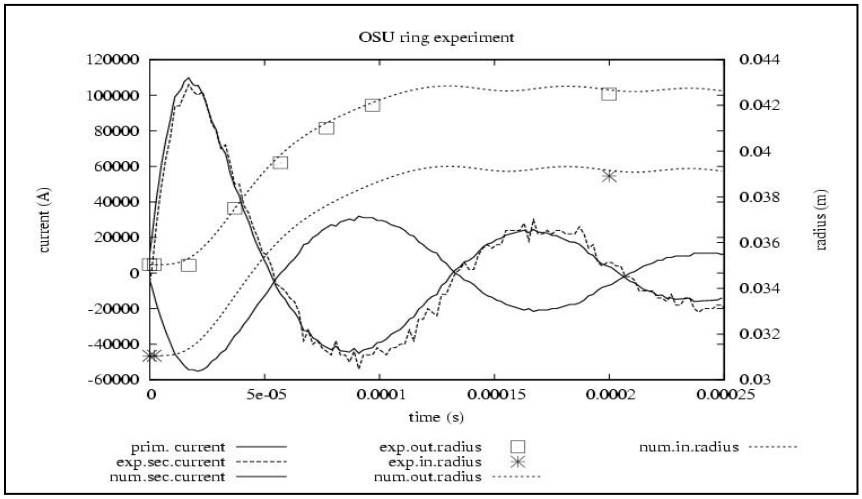

Figure 3: Experimental and numerical primary and secondary currents as well as experimental and numerical inner and outer radius of the ring vs time

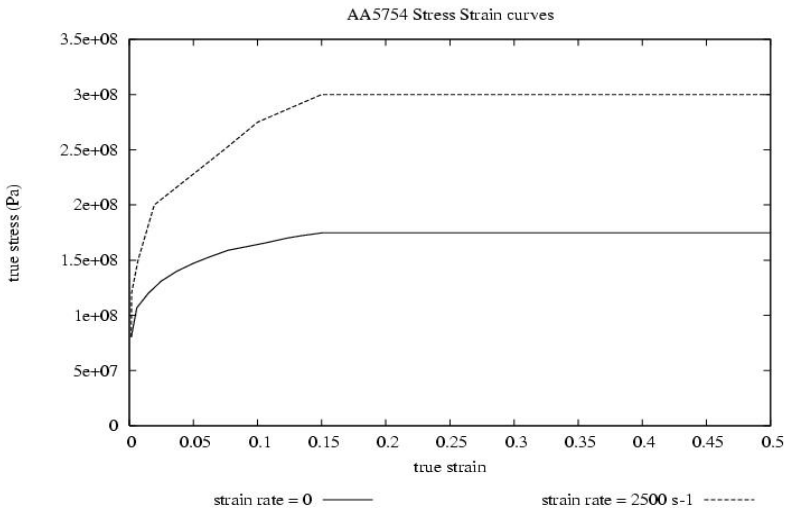

Figure 4: stress vs strain at strain rate = 0 and 2500s^{-1} for AA5754 in MAT_24 model

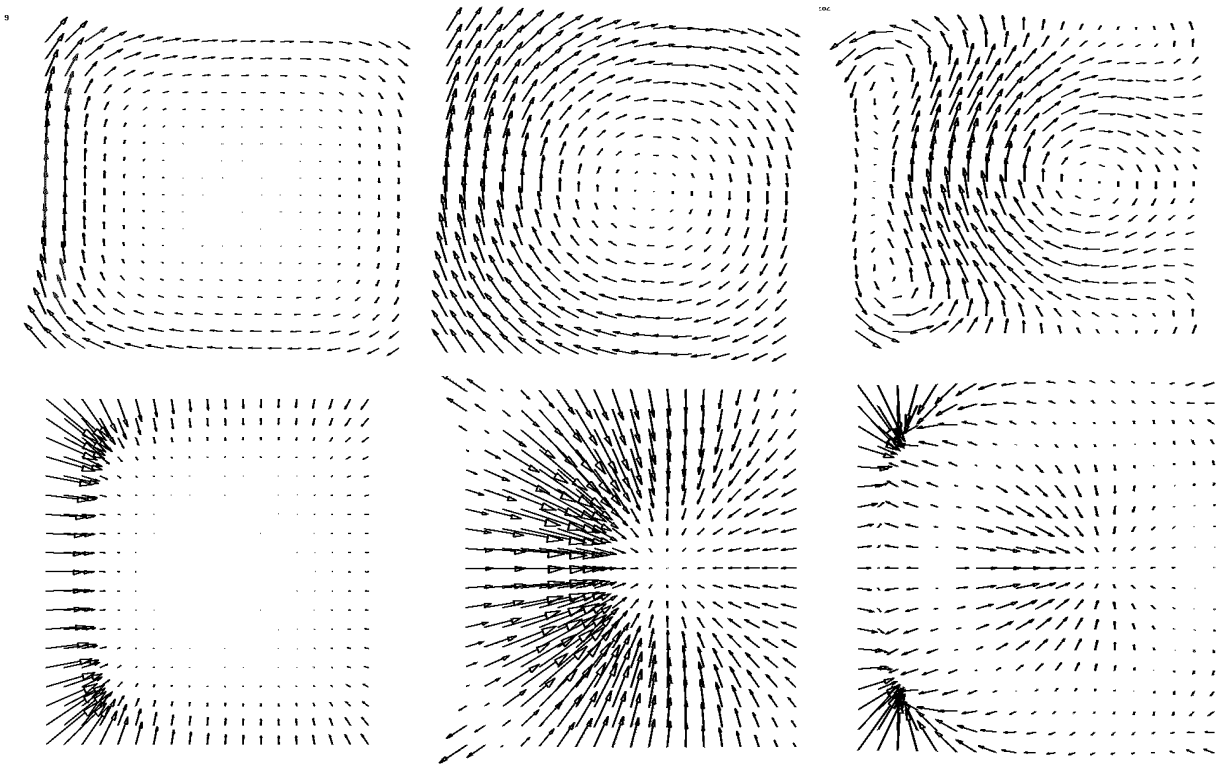

Figure 5: Magnetic field (top) and electromagnetic forces (bottom) in the cross section of the ring at three different times: t=12µs (left), t=33µs (middle) t=57µs (right). The symmetry axis is on the left of each picture.

Presentation of a typical magnetic metal forming case

The main application of magnetic metal forming is probably in sheet metal forming due to the relatively low forces needed. The electromagnetism module is thus now being extended to shell elements with some assumption for the diffusion of the magnetic field through the thickness of the shell [15]. The current density is assumed to be uniform in a given numerical “skin depth” of

the shell. Usually, this "skin depth" is taken as equal to the thickness of the shell. The assumption then means that the thickness of the shell is small compared to the actual skin depth of the problem. Detailed studies will have to be done to study the validity of this assumption, and maybe other assumptions will need to be introduced.

Meanwhile, it still is possible to use solid elements for thin plates, which allows solving the full diffusion problem. This is what we did for the second example case where the goal is to magnetically form a 0.8mm thick aluminum plate against a twisted groove shaped die. A solid mesh with 5 elements through the thickness of the aluminum shell was used. A coil with a square cross section was placed just above the shell. The diameter of the groove of the die is around 1cm, and its length around 2cm. A typical oscillating current with a 150 kA amplitude and a 20 μs quarter period is sent through the coil. This current was roughly optimized so that the workpiece hit the die without too much kinetic energy, in order not to damage the die. This is by the way the kind of optimization for which a numerical code can prove very useful. The mesh for this case, generated with TrueGrid® is presented on figure 6. It is composed of 18000 solid elements, and 2840 BEM faces.

One has to note that this mesh does not represent a full physical geometry but only a little slice of it. In an actual case, the induced current would need to loop somehow in the workpiece, and the coil would need to be connected to the line coming from the generator. For this case, the boundary conditions have been chosen such that the current can freely flow in and out the coil and the workpiece, as if they were connected to other conductors.

Figure 7 shows the iso-contours of the current density, as well as the current density and electromagnetic force density in a slice of the workpiece, at 3 different times. At the first time (t=4μs), the workpiece still is very close to the coil, and the current mainly flows in the workpiece in the area which is directly under the coil. The corresponding magnetic forces (on the right on the figure) are more or less evenly distributed in this same area. At the second time (t=20μs), the workpiece has started to move towards the die, so that the current now starts to flow where the workpiece is closest to the coil, i.e. along the edges of the groove. The corresponding magnetic forces thus start to be larger at this location. This is even more visible at the third time (t=42μs) where the forces are now concentrated on the edge of the groove. This effect helps pushing the workpiece against the edges the die later in time. The shape of the coil (which would in practice probably be composed of several parts) could be optimized to reinforce such an effect.

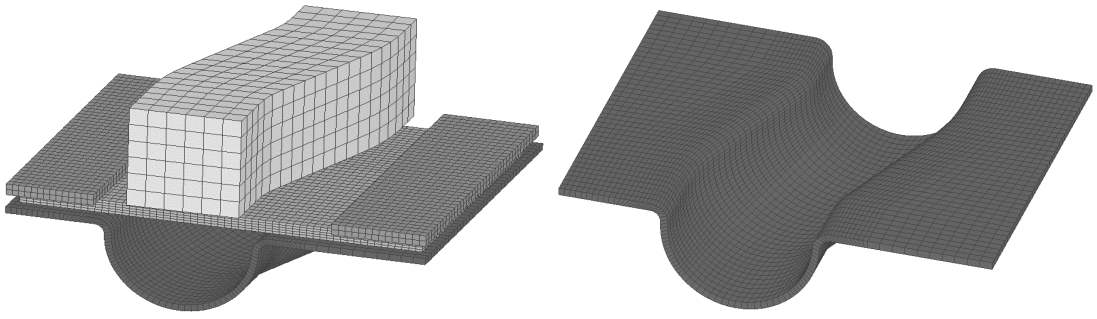

Figure 6: mesh for the magnetic metal forming example case : full mesh (left) and die only (right)

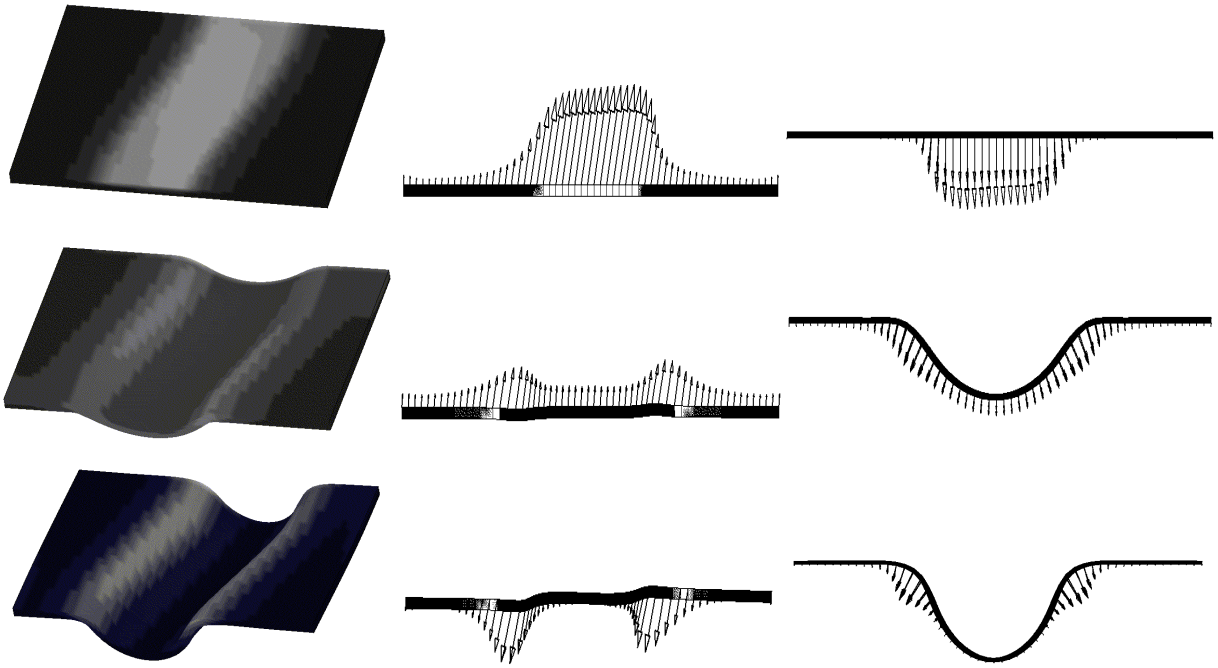

Figure 7: Iso-contours of the current density on the whole shell (left), current density on a cross section of the shell viewed from the top (middle) and electromagnetic forces on the same cross section viewed from the side (right) at 3 different times: t=4µs (top), t=20µs (middle) and t=42µs (bottom)

Conclusion

The new electromagnetism module, which is being introduced into LS-DYNA, has been briefly presented and illustrated on 2 cases. The main application of the introduction of this module and its coupling with the mechanical and thermal solvers is EMF, although many related processes can be simulated. The first validation of this module against experimental results was done on a ring expansion experiment performed at the Ohio State University. More comparisons should be done in the future. Such comparisons will not only validate the existing module, but also help understand the validity of different approximations, which may be introduced (such as the diffusion of the magnetic field through a thin shell), as well as their influence on the overall process, for each particular case.

The code can then be used for a better understanding of the physics, and in particular the evolution of the electromagnetic fields as well as the current density, the diffusion of the current and magnetic field, the induced repartition of the pressure forces, the influence of the Joule heating on the mechanical and electrical properties of the material, the part of Joule heating and plastic work in the internal energy, the time evolution of the different parts of the energy (electric, magnetic, kinetic, thermal, plastic,…), and the global yield of a given process.

The code can also be used to optimize a given process, using for example the LS-OPT optimization program. For EMF for example, the design of the coil is a very important step since its shape greatly influences the distribution of the electromagnetic fields and thus the resulting electromagnetic force. One also has to make sure that the design of the coil is such that it is mechanically strong enough to resist the large electromagnetic forces without failure or deformation.

Another very interesting application of the coupled use of LS-DYNA, LS-OPT and EMF experimental results would be in the system identification field, using a procedure which minimizes the errors with respect to given experimental results. The parameters to optimize

could for example be the ones appearing in strain rate and temperature dependent constitutive models like the Johnson-Cook [16], Zerilli-Armstrong [17] or Steinberg [18] ones, for which very little data are published. They could also be the ones appearing in the different equations of state used.

References

[1] V.S. Balanethiram, G.S. Daehn, " Hyperplasticity – Increased Forming Limits at High Workpiece Velocity", Scripta Metallurgica Et Materialia, vol. 30, pp. 515, 1994.

[2] M. Padmanabhan, "Wrinkling and Springback in Electromagnetic Sheet Metal Forming and Electromagnetic Ring Compression", The Ohio State University, 1997.

[3] C.S. Montross, T. Wei, L.Ye, G. Clark, and Y. M. Mai, "Laser Shock Processing and its Effects on Microstructure and Properties of Metal Alloys: a review", International Journal of Fatigue, Vol 24, pp1021,1036, 2002.

[4] Z. Ren and A. Razek, "New techniques for solving three-dimensional multiply connected eddy-current problems", IEE Proceedings, Vol 137, Pt. A, No3, May, 1990.

[5] P. Castillo, R. Rieben, and D. White, "FEMSTER: An Object Oriented Class Library of Discrete Differential Forms", Proceedings of the 2003 IEEE International Antennas and Propagation Symposium, volume 2, pp 181-184, Columbus, OH, June 2003.

[6] P. Castillo, J. Koning, R. Rieben, M. Stowell and D White, "Discrete Differential Forms: A Novel Methodology for Robust Computational Electromagnetism", Lawrence Livermore National Laboratory Report UCRL-ID-151522, January 2003.

[7] R. Rieben, "A Novel High Order Time Domain Vector Finite Element Method for the Simulation of Electromagnetic Device", Ph.D. dissertation, University of California at Davis, Livermore, CA 2004, UCRL-TH-205466.

[8] M. Seth and G. S. Daehn, "Effect of Aspect Ratio on High Velocity Formability of Aluminum Alloy", Trends in Materials and Manufacturing Technologies for Transportation Industries, edited by TMS (The Minerals, Metals and Materials Society), 2005.

[9] D.A. Oliveira, "Electromagnetic Forming of Aluminum Alloy Sheet: Experiment and Model", Thesis, University of Waterloo, Ontario, Canada, 2002.

[10] T.J. Burgess, "Electrical resistivity model of metals", 4th International Conference on Megagauss Magnetic-Field Generation and Related Topics, Santa Fe, NM, USA, 1986

[11] www.pearsonelectronics.com

[12] www.rocoil.cwc.net

[13] www.cookecorp.com

[14] M. Seth, Ph.D. Thesis, "Factors Affecting High Velocity Formability", (2006).

[15] Z. Ren and A. Razek, "A Coupled Electromagnetic-Mechanical Model for Thin Conductive Plate Deflection Analysis", IEEE Transactions on Magnetics, vol. 26 No 5, September 1990.

[16] G.R. Johnson, and W.H. Cook, "Fracture Characteristics of Three Metals Subjected to Various Strains, Strain Rates, Temperatures and Pressures", Engineering Fracture Mechanics, Vol 21, No 1, pp 31-48, 1985.

[17] F.J. Zerilli and R.W. Armstrong, "Dislocation-mechanics-based constitutive relations for material dynamics calculations", J.Appl.Phys. 61(5), 1March 1987

[18] D.J.Steinberg, S.G.Cochran, M.W.Guinan, A Constitutive Model for Metals Applicable at High-Strain Rate, J.Appl.Phys.51,1498 (1980)